Journal of Hydrology 617 (2023) 128989

Contents lists available at ScienceDirect

Journal of Hydrology

journal homepage: www.elsevier.com/locate/jhydrol

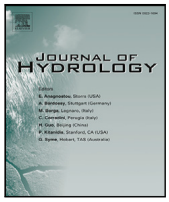

Research papers

Identifying discontinuities of flood frequency curves

Arianna Miniussi [a,b], Ralf Merz [a,c], Lisa Kaule [a,d], Stefano Basso [a,e,*]

[a] Department of Catchment Hydrology, Helmholtz Centre for Environmental Research - UFZ, Halle (Saale), Germany
[b] General Reinsurance, Cologne, Germany
[c] Institute of Geosciences and Geography, Martin-Luther University Halle-Wittenberg, Halle (Saale), Germany
[d] Department of Hydrology, University of Bayreuth, Bayreuth, Germany
[e] Norwegian Institute for Water Research (NIVA), Oslo, Norway

ARTICLE INFO

This manuscript was handled by Marco Borga, Editor-in-Chief, with the assistance of Nadav Peleg, Associate Editor.

Keywords:
Extreme floods
Flood hazard
Flood divide
Flood frequency curves
Physically-based framework
Detection method

ABSTRACT

Discontinuities in flood frequency curves, here referred to as flood divides, hinder the estimation of rare floods. In this paper we develop an automated methodology for the detection of flood divides from observations and models, and apply it to a large set of case studies in the USA and Germany. We then assess the reliability of the PHysically-based Extreme Value (PHEV) distribution of river flows to identify catchments that might experience a flood divide, validating its results against observations. This tool is suitable for the identification of flood divides, with a high correct detection rate especially in the autumn and summer seasons. It instead tends to indicate the emergence of flood divides not visible in the observations in spring and winter. We examine possible reasons of this behavior, finding them in the typical streamflow dynamics of the concerned case studies. By means of a controlled experiment we also re-evaluate detection capabilities of observations and PHEV after discarding the highest maxima for all cases where both empirical and theoretical estimates display flood divides. PHEV mostly confirms its capability to detect a flood divide as observed in the original flood frequency curve, even if the shortened one does not show it. These findings prove its reliability for the identification of flood divides and set the premises for a deeper investigation of physiographic and hydroclimatic attributes controlling the emergence of discontinuities in flood frequency curves.

1. Introduction

Despite considerable efforts to achieve reliable estimation of rare floods, these events are still among the most common natural disasters (Wallemacq and House, 2018). The evaluation of their hazard is however crucial for several applications, including the design of hydraulic structures, risk planning and mitigation, and computation of premiums in the insurance industry. Appraisal of the flood hazard is especially difficult when the magnitude of the rarer floods can take values which are several times to orders of magnitude larger than commonly observed floods, resulting in a marked uprise of the flood frequency curve beyond certain return periods (Rogger et al., 2012; Smith et al., 2018).

Cognitive biases often lead to downplay the occurrence of such extreme events (Merz et al., 2015, 2021), although the scientific literature repeatedly signaled the pervasiveness of these behaviors terming them in various ways. In fact, heavy-tailed distributions of floods (Farquharson et al., 1992; Bernardara et al., 2008; Villarini and Smith, 2010), inversions of concavity and step changes in flood magnitude–frequency curves (Rogger et al., 2012; Guo et al., 2014; Basso et al., 2016) and large values of the ratios between the maximum flood of record and the sample flood with a specified recurrence time (Smith et al., 2018) and between empirical high flow percentiles (Mushtaq et al., 2022) are all manifestations of a marked increase of the magnitude of the rarer floods highlighted by means of different approaches. To further stress the common nature of all these phenomena, in this study we favor none of the previous locutions and instead label them as *flood divides*. The term was chosen to highlight the existence of a discharge threshold which marks the rise of progressively larger floods (red square in Fig. 1d) and thus distinguishes between common and increasingly extreme floods that may occur in river basins.

Rogger et al. (2012) investigated marked uprises (i.e., discontinuities in the slope) of flood frequency curves, which they called step changes, by leveraging information collected from field surveys in two small alpine catchments to calibrate a distributed deterministic rainfall-runoff model. They suggested that step changes occur when a threshold of the catchment storage capacity is exceeded, and performed a synthetic experiment (Rogger et al., 2013) to examine the effect of catchment storage thresholds and combined multiple controls

* Corresponding author at: Norwegian Institute for Water Research (NIVA), Oslo, Norway.
E-mail address: stefano.basso@niva.no (S. Basso).

https://doi.org/10.1016/j.jhydrol.2022.128989
Received 8 February 2022; Received in revised form 26 November 2022; Accepted 4 December 2022
Available online 20 December 2022

(e.g., the temporal variability of antecedent soil storage and the size of the saturated regions) on the return period of the step change. They also highlighted important implications of the presence or absence of flood divides for estimation and design purposes, further stressing the need for a robust method to identify their possible occurrence. In fact, misidentifying the presence of flood divides may either lead to overestimation of rare floods (if large recorded outliers are considered in the analyses) or to their underestimation, in case events larger than the flood divide were not yet recorded or are regarded as outliers.

Guo et al. (2014), Basso et al. (2016) instead linked different shapes of flood frequency curves and a marked growth of the magnitude of the rarer floods to the catchment water balance. The former justified these features through the aridity index (i.e., the ratio between mean annual potential evaporation and precipitation, Budyko (1974)), showing that flood frequency curves characterized by increasing aridity index are steeper. The latter explained them by means of the persistency index (i.e., the ratio between mean catchment response time and runoff frequency, Botter et al. (2013)) and highlighted that the concavity of the flood frequency curve changes from downward to upward shifting from persistent to erratic regimes, thus causing the emergence of flood divides.

Smith et al. (2018) computed the ratio between the maximum flood of record and the sample 10-year flood for thousands of gauges across the USA, finding large values for a substantial amount of them. Different flood-generating processes (Merz and Blöschl, 2003; Berghuijs et al., 2014; Tarasova et al., 2020) or mixtures of flood event types (Hirschboeck, 1987; Villarini and Smith, 2010; Smith et al., 2018) were indicated by other studies as possible causes of these marked increases of the magnitude of the rarer floods.

Finally, a rather common approach to study this phenomenon consists in evaluating the shape parameter of Generalized Extreme Value distributions fitted to observed annual maximum series (Farquharson et al., 1992; Bernardara et al., 2008; Villarini and Smith, 2010; Smith et al., 2018). Notwithstanding the drawbacks of such a parametric approach applied in association with limited records of annual maxima, these studies highlighted the ubiquitous occurrence of flood divides and flood distributions characterized by thick upper tails, as indicated by widespread positive values of the shape parameter. Moreover, Smith et al. (2018) showed that the values of the shape parameter significantly increase with longer data records. Their findings thus suggest that uprises of flood frequency curves may be the norm rather than rare conditions, pointing to the limited data record as the reason for the latter belief.

Although former research hints at the ubiquitousness of flood divides in flood frequency curves and provide indications of their possible drivers, a quantitative methodology to identify flood divides, which is robust to sampling uncertainty and tested in a large set of case studies, is still lacking. The relevance of our study is thus twofold: (i) we develop such a methodology for the detection of flood divides and evaluate their emergence across the US and Germany, in a large set of catchments with contrasting physio-climatic features; (ii) we examine the reliability of a process-based stochastic framework for the estimation of flood frequency curves to detect flood divides and infer their occurrence, benchmarking its results against observations.

2. Methodology and data

2.1. The physically-based Extreme Value distribution of river flows

2.1.1. Theoretical framework

The PHysically-based Extreme Value (PHEV) distribution of river flows is a parsimonious mechanistic–stochastic formulation of flood frequency curves (Basso et al., 2016, 2021) that stems from a rigorous mathematical description of catchment-scale daily soil moisture and streamflow dynamics in river basins (Laio et al., 2001; Porporato et al., 2004; Botter et al., 2007). In this framework, daily precipitation is represented as a marked-Poisson process with frequency λ_P $[T^{-1}]$ and exponentially-distributed depths with average value α $[L]$. Soil moisture decreases due to evapotranspiration and is replenished by precipitation events that eventually trigger runoff pulses when an upper wetness threshold is crossed. These pulses, which feed water to a hydrologic storage, are also a Poisson process with frequency $\lambda < \lambda_P$ $[T^{-1}]$ and an exponential distribution of magnitudes with mean α $[L]$. A non-linear (i.e., power-law) storage-discharge relation with parameters a and K epitomizes the hydrological response of the catchment and encompasses the joint effect of different flow components (Brutsaert and Nieber, 1977; Basso et al., 2015b).

The above-summarized mechanistic–stochastic description of runoff generation processes allows for expressing the probability distributions of daily flows (Botter et al., 2009) and peak flows (i.e., local flow peaks occurring as a result of streamflow-producing rainfall events) as a function of a few physically meaningful parameters (Basso et al., 2016). It also enables characterizing hydrologic regimes according to their typical streamflow dynamics, which are summarized by the persistency index (Botter et al., 2013). This is defined as the ratio between runoff frequency and the mean hydrograph recession rate, i.e., $\frac{\lambda}{K(\alpha\lambda)^{a-1}}$ (Basso et al., 2016; Deal et al., 2018).

An erratic regime (lower values of the persistency index), which is commonly found during dry seasons, very hot humid seasons with intense evapotranspiration or in fast responding catchments, is characterized by periods between the arrival of runoff-producing rainfall events which are longer than the typical duration of flow pulses. Conversely, a persistent regime (higher values of the persistency index), typically occurring in cold-humid seasons and lowland catchments, is characterized by frequent rainfall events and a rather constant water supply to the catchment.

Considering that peak flows in a given reference period (e.g., a season) are Poisson distributed and postulating their independence yield the probability distribution of flow maxima (i.e., maximum values in a specified timespan). The return period is finally obtained as the inverse of the exceedance cumulative probability of flow maxima, thus providing an expression of the flood frequency curve which reads (Basso et al., 2016):

$$T_r(q) = \frac{1}{1 - exp\left[-\lambda\tau D_j(q)\right]} \tag{1}$$

where τ [T] is the duration in days of the reference period used in the analyses; $D_j(q) = \int_q^\infty p_j(q)\,dq$ is the exceedance cumulative probability of peak flows; p_j is the probability density function of peak flows, $p_j(q) = Cq^{1-a}\exp(\frac{\lambda q^{1-a}}{K(1-a)} - \frac{q^{2-a}}{\alpha K(2-a)})$; α and λ are the aforementioned parameters describing Poisson-distributed runoff events, a and K are the parameters of the power-law storage-discharge relation, and C is a normalization constant.

2.1.2. Parameter estimation

The four parameters of PHEV (α, λ, a, K) are rather straightforward to estimate at the catchment scale. They are indeed directly derived from the observed time series of precipitation and streamflow: α is computed as the mean daily rainfall depth in rainy days, while λ (frequency of streamflow-producing rainfall) as the ratio between the long term mean daily flow $\langle q \rangle$ and α (Botter et al., 2007). The parameters of the power-law storage-discharge relation (i.e., the recession exponent a and coefficient K) are estimated through hydrograph recession analysis (Brutsaert and Nieber, 1977) following the approach proposed by Biswal and Marani (2010). Finally, the recession coefficient is not directly used as input in Eq. (1), but it is replaced by its maximum likelihood estimation on the observed seasonal flood frequency curve (Basso et al., 2016).

2.2. Identification of flood divides

To identify flood divides, we start from the method proposed by Rogger et al. (2013): a flood divide is defined as the sharpest bend of the flood frequency curve, here considered in terms of rescaled streamflow maxima (i.e., seasonal maxima divided by the long term mean daily flow, $\langle q \rangle$) as a function of the return period, the latter represented in logarithmic scale. We then develop a new methodology dedicated to its identification from both empirical estimates of the flood frequency curve obtained by means of Weibull plotting position and models, such as PHEV.

The resulting approach, which can be employed without depending on subjective evaluation, is detailed in the following.

1. The curvature of the flood frequency curve, of which we show an example in Fig. 1, is computed as $logTr''/(1+logTr'^2)^{(3/2)}$ (where the apex indicates the derivation operation with respect to the rescaled streamflow) for both the observations and PHEV. In the former case, we use the method developed by Jianchun et al. (1995) for computing derivatives in non-equally spaced points, while for PHEV we employ the Python routine from the Scipy library (*misc.derivative*), which uses a central difference formula with spacing dx to compute the n^{th} derivative at a specified point.
2. As the noise associated to computing the curvature on a discrete and rather sparse set of points (seasonal maxima) might lead to identification errors, a heuristic filter is applied on the curvature calculated from observations: only points on the right-hand side of the last value of the curvature exceeding the range $\pm\sigma$ (where σ indicates the standard deviation of the curvature itself) are considered (Fig. 1c).
3. The Mann–Whitney U-test (Mann and Whitney, 1947) is applied on the values of the first derivatives on the left and right-hand sides of each potential flood divide identified at point 2 to check if their distributions are statistically different at a significant level equals to 0.05 (in other words, if the slope of the curve significantly differs between the left and right-hand side of the flood divide); the effect size is then computed by means of the Cohen's d (Cohen, 1974) to evaluate if the magnitude of the difference is relevant (Sullivan and Feinn, 2012). For PHEV, this step is performed on a dense set of values, equally spaced with an interval $\Delta q = 0.05$ up to a value of rescaled streamflow equal to 200, i.e., 200 times the long-term average streamflow. The relative increment of the slope between the left and right-hand side of a potential PHEV flood divide is also evaluated within the observational range.
4. We finally identify as flood divide the point for which the p-value of the Mann–Whitney test is the lowest, provided that the Cohen's d is greater than 0.4 (moderate effect size; (Gignac and Szodorai, 2016; Lovakov and Agadullina, 2021)) and the slope increment exceeds a value of 1%.

Fig. 1 visually exemplifies the application of the developed approach for flood divides detection to the flood frequency curve of the Rott river at Kinning, Bavaria (ID: 18801005), in the summer season. In Fig. 1a the flood frequency curve is represented with switched axes (i.e., the logarithm of the return period is represented on the y-axis whereas the rescaled seasonal maxima on the x-axis), as streamflow is the independent variable in Eq. (1). The red square in Fig. 1a, d represents the selected flood divide, i.e., the one associated to the lowest p-value of the Mann–Whitney U-test applied to the distributions of the first derivatives (Fig. 1b) and fulfilling the additional criterion on the Cohen's d. We also show points that are initially analyzed as potential flood divides (i.e., all the points with a Mann–Whitney p-value lower than 0.05, orange squares in Fig. 1a).

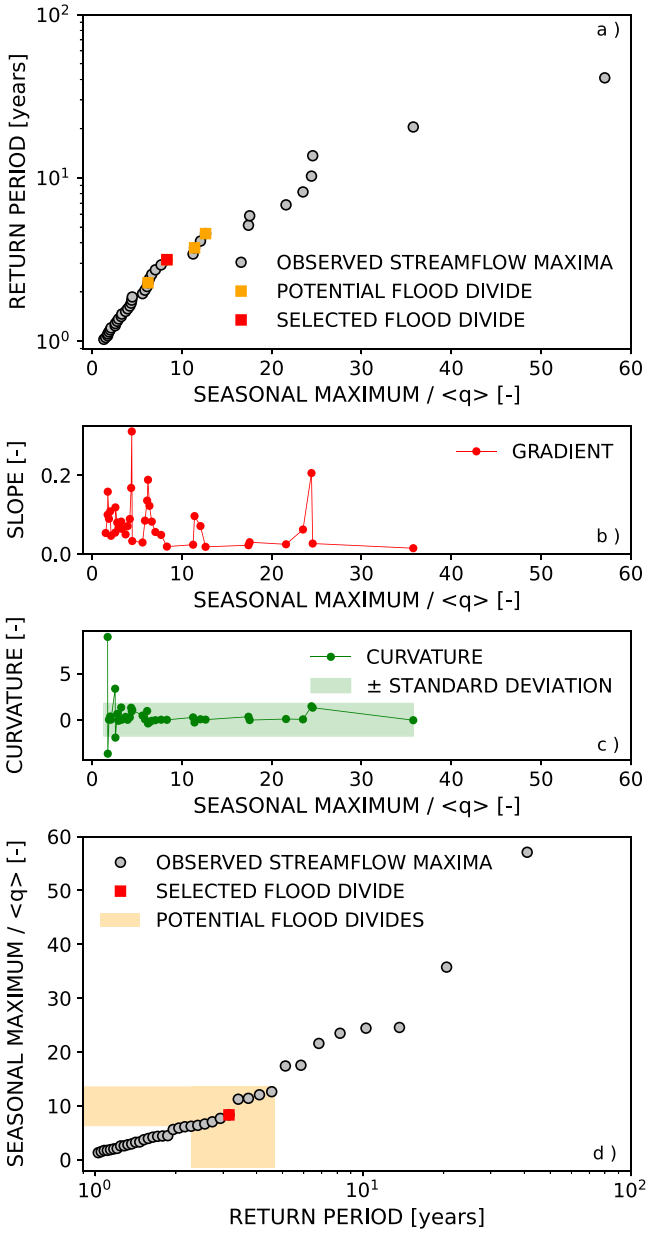

Fig. 1. Exemplary application of the proposed methodology to detect flood divides to the Rott river at Kinning, Bavaria (ID: 18801005), in the summer season. (a) Visualization of how the approach is actually applied, i.e., expressing the logarithm of the return period as a function of the rescaled seasonal maxima (gray filled circles). Potential flood divides (i.e., all the points with a p-value of the Mann–Whitney U-test lower than 0.05) are represented by orange squares, while the selected one (i.e., the one exhibiting the minimum p-value of the Mann–Whitney U-test and Cohen's d greater than 0.4) is depicted with a red square. (b) First derivative computed on observations. (c) Curvature computed on observations, with the shaded area representing twice its standard deviation. (d) Standard representation of the flood frequency curve, namely observed maxima as a function of the logarithmic value of the return period (gray filled circles). The red square indicates the selected flood divide, while the orange shaded area represents the range of potential flood divides. (For interpretation of the references to color in this figure legend, the reader is referred to the web version of this article.)

2.3. Datasets

We use daily rainfall and streamflow time series from the Model Parameter Estimation Experiment dataset (MOPEX, data from 1948 to 2003) (Duan et al., 2005; Schaake et al., 2006) and from Germany (1951–2013) (Tarasova et al., 2018). Streamflow is measured at the gauging stations whose geographical coordinates are listed in Table S1, whereas the corresponding rainfall records are spatially averaged

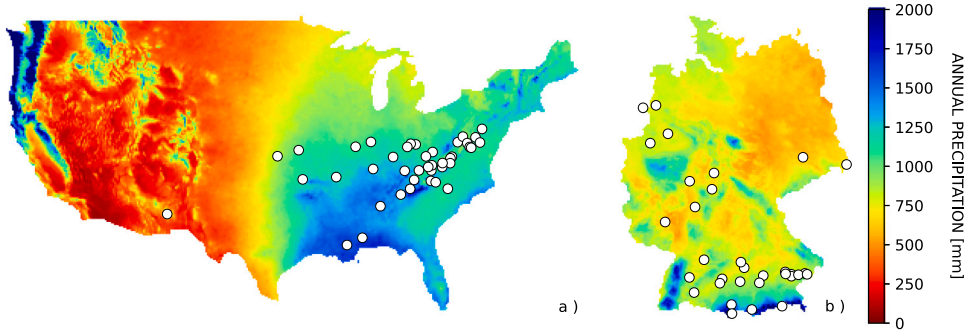

Fig. 2. Select river basins (white filled circles) from the (A) MOPEX and (B) German datasets. The background of the maps represents 30-years annual precipitation normals (1981–2010 for the US and 1991–2020 for Germany). (For interpretation of the references to color in this figure legend, the reader is referred to the web version of this article.)

values for the upstream drainage areas derived from gridded datasets. We perform all analyses in a seasonal time frame (spring: March to May; summer: June to August; autumn: September to November; winter: December to February) to account for the seasonality of rainfall and runoff (Allamano et al., 2011; Baratti et al., 2012). To assure that PHEV suitably represents the key processes of streamflow generation in the set of case studies, we only consider catchments with low human impact, weak or absent inter-seasonal snow dynamics (Botter et al., 2013; Wang and Hejazi, 2011) and hydrograph recession properties which are independent of the peak flow (Basso et al., 2021). Similarly to previous studies (Merz et al., 2020), we as well restrict our analysis to cases for which the root mean square error ($RMSE$) between the predicted and observed flood frequency curve is limited (i.e., lower than 0.3), as a fairly accurate estimation of the flood frequency curve is a precondition to investigate if PHEV is able to correctly identify flood divides and whether their occurrence is affected by physio-climatic catchment attributes. Figure S1 provides a summary of the performance of PHEV (quantified by means of varied error metrics, see Supplementary Material) in reproducing observed flood frequency curves in the considered set of case studies. This selection yields a set of 101 case studies (i.e., catchment-season combinations), divided into 23, 29, 23 and 26 cases respectively in the spring, summer, autumn and winter seasons. The median length of the considered data series is 54 years (min: 34, max: 55) for the MOPEX and 58 years (min: 40, max: 63) for the German case studies. Their catchment areas vary between 43 and 9052 km^2 (median: 865 km^2). The locations of their outlets are displayed in Fig. 2.

3. Results and discussion

We apply the methodology for the identification of flood divides introduced in the previous section to each observed and analytic seasonal flood frequency curve, thus allowing for evaluating the flood divide detection of PHEV against observations, which we consider as benchmark (Fig. 3). The bar plots in Fig. 3 show the percentages of case studies for which a flood divide is identified from both PHEV and the observational records (true positives, dark green color), those which display a flood divide neither in the empirical nor in the analytic flood frequency curves (true negatives, light green), the percentages of cases where a flood divide is detected from the observations but not from the analytical model (false negatives, red), and those where the analytical model has foreseen the occurrence of a flood divide which is not confirmed by the available observations (false positives, orange). The existence of both true positives and true negatives emphasizes the capability of PHEV to mimic varied observed shapes of flood frequency curves (Basso et al., 2016) and to identify both the presence and the absence of a flood divide.

The bar plots in Fig. 3a and 3b differ for the criteria applied in the flood divide identification methodology. In Fig. 3a only the controls on the p-value of the Mann–Whitney U-test mentioned in Section 2.2 are considered, whereas the additional requirements on the effect size and slope increment are as well used in Fig. 3b. True positives (dark green) prevail in the summer (18 cases) and autumn (14 cases) seasons of Fig. 3a, amounting to about 60% of the cases. False positives constitute instead a sizable share of the cases in spring (12 cases) and winter (21 cases). When more stringent requirements for the identification of flood divides are used, by accounting for the mentioned additional criteria, the percentage of true positives decreases (Fig. 3b, dark green; respectively 3, 11, 12 and 1 cases in spring, summer, autumn and winter). A few cases of those shifting category become true negatives (for an overall number of 2, 3, 1 and 1 cases in spring, summer, autumn and winter), indicating that the slope of the flood frequency curve does not substantially increases on the right-hand side of the potential flood divide, thus not representing a noteworthy hazard. Most of them however become false positives (orange color in Fig. 3b; respectively 18, 15, 9 and 24 cases in spring, summer, autumn and winter) as the identified changes of the slope of the observed flood frequency curve are not substantial according to the limited amount of available observations, whereas PHEV confirms the existence of a flood divide thanks to its evaluation in an unlimited number of points. Consistent results are also found when considering different significant levels for the Mann–Whitney test: the strictest the level the highest the share of cases shifting between true and false positives, which once again points to the unfeasibility of detecting flood divides with confidence from plain observations.

The predominance of false positives in spring (18 cases) and winter (24 cases) (orange color in Fig. 3b) calls for further investigation of their causes. We therefore hypothesize that PHEV, by leveraging the embedded mechanistic description of hydro-climatic dynamics taking place in watersheds and the information gained from analyzing daily rainfall and streamflow series, might indicate the possible emergence of flood divides that are not yet displayed by the observed flood frequency curves. In fact, these empirical estimates are likely affected by small sizes of the samples of large events (i.e., those on the right-hand side of each potential flood divide, see Fig. 1a) and by the specific character of catchments, which may have a more or less enhanced propensity to exhibit extreme floods and thus display them in a limited data record. We then perform the following experiment to test this hypothesis. We consider the set of true positives (i.e., the 27 cases for which both PHEV as well as the observed flood frequency curve show a flood divide) and retain only maxima with return periods below 5 years (see an explanatory example in Fig. 4a, where the maxima retained are represented by gray filled circles with blue contours). In so doing, we approximately discard in each case the largest ten points and their corresponding years of occurrence. Thereby, fictitious flood frequency curves only comprising maxima with smaller magnitudes (and return periods) are created, thus reproducing the conditions we hypothesized as possible reasons of the emergence of false positives. We then apply the usual methodology for identifying flood divides on these fictitious flood frequency curves and the corresponding shortened data records.

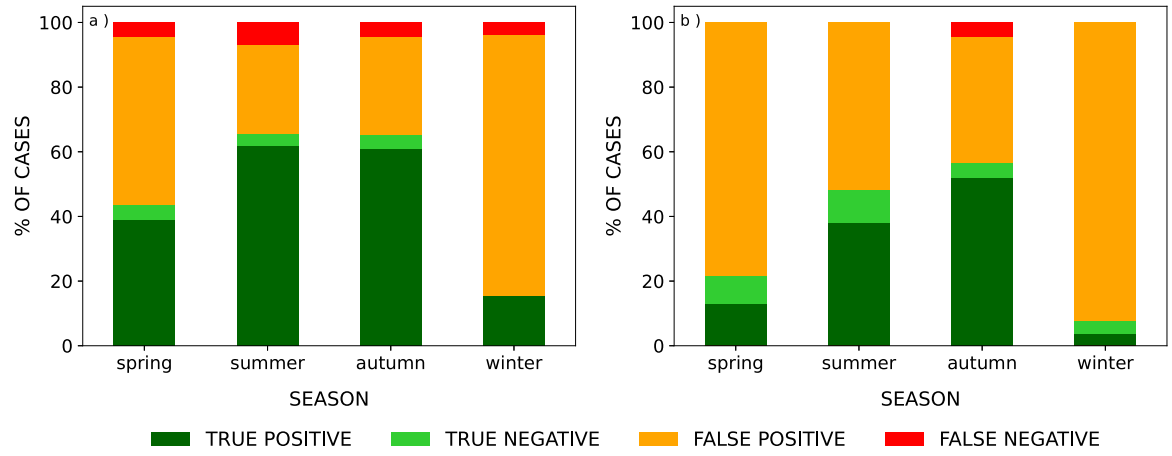

Fig. 3. Performance of the PHysically-based Extreme Value (PHEV) distribution of river flows in the detection of flood divides when only the controls on the Mann–Whitney U-test are considered (see Section 2.2, panel a) and when the whole methodology for detecting flood divides is applied (see Section 2.2, panel b). Percentages are calculated on the overall number of case studies, which amount to 23, 29, 23 and 26 cases respectively in the spring, summer, autumn and winter seasons. True positives (dark green color; 27 cases in panel b) and true negatives (light green; 7 cases) indicate coherence between PHEV and observations, i.e., flood divides are either detected or not from both PHEV and the observed records. These constitute a large number of cases in summer (14 cases) and autumn (13 cases). False positives (orange; 66 cases) and false negatives (red; 1 case) represent the cases in which either PHEV detects a flood divide that was not identified by the observations or the observations display a flood divide which is not detected by PHEV. The indicated absolute numbers of positive and negative cases refer to the complete application of the methodology for detecting flood divides (i.e., panel b). The reasons for the presence of false positives are further investigated in the study and clarified in the text and figures. (For interpretation of the references to color in this figure legend, the reader is referred to the web version of this article.)

PHEV detects a true flood divide (i.e., true positives) in 81% of the cases (22 case studies) even when the largest points are removed, whereas the observations only in 40% (11 cases). The maps in Fig. 4b and 4c summarize this result: half circles are colored either in green, if a flood divide is successfully detected from the shortened flood frequency curve, or in red in the opposite case. The left half of the circle depicts the detection capability of PHEV, while the right side the results obtained from the observations. It can be easily seen that most left halves of the circles are colored in green and most of the right ones are instead red, thus indicating a high success rate of PHEV and a significantly lower one of observations in inferring the emergence of flood divides from shortened records. A similar result is obtained by discarding maxima with return period greater than 10 years (i.e., discarding about five-six points instead of the highest ten), when PHEV correctly detects 85% of true flood divides (23 cases) in comparison to a correct detection rate from observations of 60% (16 cases). The outcome of this experiment strongly suggests that the detected false positives (orange color in Fig. 3) indeed arise because of the statistical uncertainty of limited data records and the capability of PHEV to infer the occurrence of flood divides from short series rather than by its inability to correctly identify inflection points which were detected (or not) in the observed flood frequency curves.

A physical explanation of the reason why some observational series might not exhibit a flood divide which shall be expected is provided by considering typical streamflow dynamics occurring for distinct river flow regimes, here characterized by means of the persistency index (Botter et al., 2013). When streamflow values weakly oscillate around their mean (persistent regimes), the probability of occurrence of relatively large flows is very low, and extreme events are unlikely to be captured by short time series. On the contrary, erratic regimes are composed of a sequence of high flows interspersed in between prolonged periods of low flows. Events which are several times (i.e., order of magnitudes) higher than the average flow are thus more likely to occur in these regimes (Basso et al., 2015a). In the context of this study, false positives shall therefore mostly occur for persistent regimes, as such large events enabling detection of flood divides from empirical flood frequency curves are less likely to have been observed during the available data record.

Fig. 5a displays the percentages of true positives (dark green color; from left to right: 9, 10, 6, 2 and 0 cases), true negatives (light green; respectively 5, 1, 0, 0, 1 cases), false negatives (red; 1, 0, 0, 0, 0 cases) and false positives (orange; from left to right: 6, 9, 14, 18 and 19 cases) for five ranges of the persistency index set so as to have an equal number of values (~20) per bin. The number of false positives consistently increases with the persistency index, thus corroborating the above reasoning. No clear patterns are instead observed with, e.g., the drainage area and the average rainfall magnitude in the catchment (Figure S3), which are sometimes regarded as possible drivers of a marked increase of the magnitude of the rarer floods (Gaume, 2006; Villarini and Smith, 2010).

A recent review of the current scientific knowledge (Merz et al., 2022) suggests explanations for these results. It signals an unlikely direct role of catchment size in determining tail behaviors of flood distributions, as increasing drainage areas entail both spatial aggregation (which may cause lighter tails), and shifts of dominant processes (e.g., different precipitation types and runoff generation mechanisms) which may lead in the opposite direction. It also reports robust evidences against a dominant role of rainfall characteristics for the emergence of heavy-tailed flood distributions, as runoff generation processes strongly modulate the hydrologic response. On the contrary, the available literature emphasizes the role of non-linear hydrological responses and the catchment water balance for the emergence of heavy tails. These are the two key processes described by PHEV and summarized by the persistency index, which thus arises as a pivotal indicator of the possibility to detect flood divides from data records.

To further highlight the relation between typical river flow dynamics recapped in the persistency index and the occurrence of false positives we compare in Fig. 5b the cumulative distributions of the persistency index for true cases (green) and false positives (orange). The distributions clearly differ. True cases feature more erratic regimes which facilitate their identification from data records, whereas false positives mostly occur for persistent regimes. This qualitative evaluation is validated by applying the 2-sample Kolmogorov–Smirnov test, which evaluates if two samples come from the same distribution (null-hypothesis), to the sets of true and false positives (the same is obtained by comparing true negatives and false positives). We can reject the null-hypothesis at the 0.01 significance level, meaning that the two samples are drawn from different distributions and false positives are significantly more likely to occur for persistent regimes. The same cannot be proved for the cumulative distributions of catchment area (p-value = 0.44) and average rainfall magnitude (p-value = 0.34) for the sets of true and false positives. Remarkably, the seasons characterized

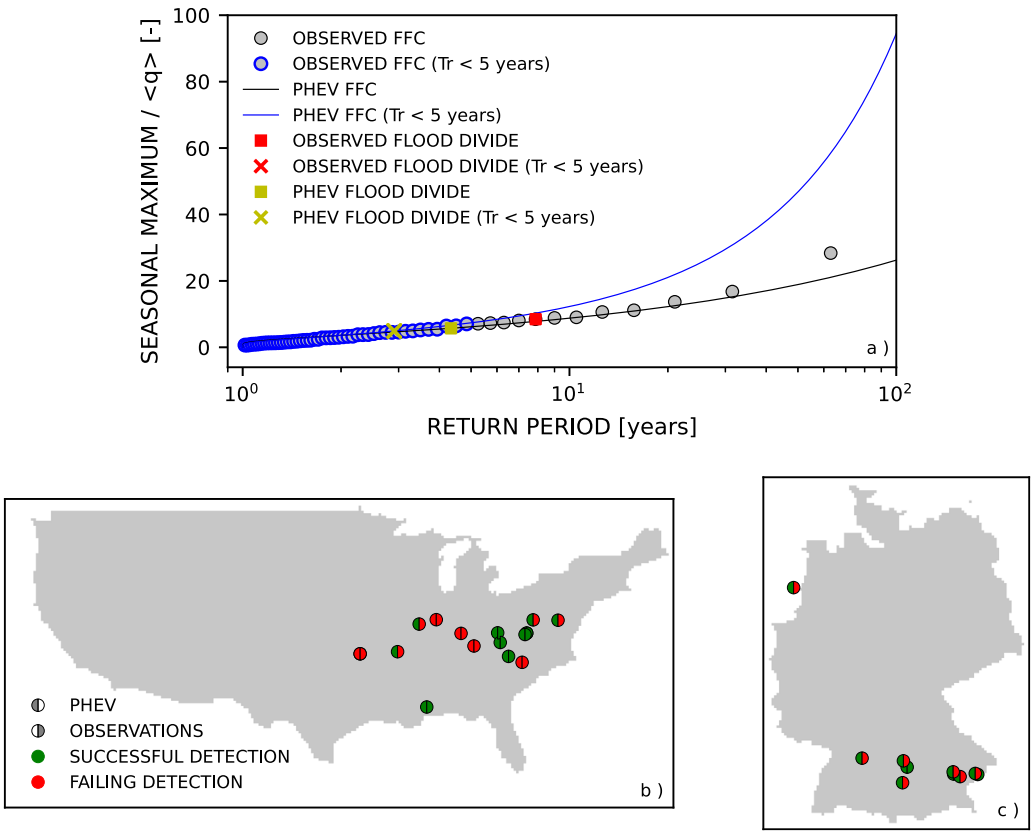

Fig. 4. Visual explanation and results of an experiment aimed at testing hypotheses on the emergence of false positives. (a) Gray dots with black (blue) contour represent the complete (shortened, until a return period of 5 years) observed seasonal maxima series of the Wörnitz river at Harburg, Bayern (ID:11809009), in the summer season. The solid black (blue) line displays the analytic flood frequency curve (i.e., PHEV) whose parameters are estimated from the complete (shortened) time series. The red (yellow) square indicates the flood divide detected from the observations (by PHEV) using the complete series, while the corresponding crosses (the red one is not visible in the plot as no flood divide was detected after shortening the observations) represent the observed and analytic flood divides detected on the shortened flood frequency curve. (b–c) Locations of the true positives in the US (panel b) and Germany (panel c). The left (right) half of the circles represent PHEV (observations) ability to detect a flood divide when the shortened flood frequency curves (i.e., maxima characterized by return period below 5 years) are used. The green (red) colored halves indicate successful (failing) detection. Remarkably, most of the left halves are green (PHEV detects true flood divides even from the shortened series in the majority of the cases), whereas most of the right ones are red (flood divides are not always identified from observations when the shortened records are used). (For interpretation of the references to color in this figure legend, the reader is referred to the web version of this article.)

by the larger portion of false positives are spring and winter, during which regimes tend to be more persistent.

The physical explanation provided here of the different telling power of streamflow data for rivers characterized by distinctively different streamflow dynamics agrees with the results of previous research. For example, Botter et al. (2013) showed less variable streamflow distributions across years in erratic regimes compared to persistent ones, which determines higher representativeness of their estimates in the former case for a given length of the data record. Smith et al. (2018) also demonstrated that upper tail ratios grow with the length of data and, for a given data length, are larger (i.e., flood divides are more often identified) in arid and semiarid regions than in humid ones. Their results jointly suggest that, given similarly long data records, the typical (erratic) flow dynamics of drier areas enable more reliable characterization of the whole range of values possibly spanned by streamflow and of the presence or absence of flood divides according to the physical explanation provided above.

4. Concluding remarks

In this work we examine the occurrence of marked uprises of flood frequency curves (termed flood divides), which are pivotal for a correct estimation of river flood hazard. We develop a robust methodology to identify them from observational records and models, and evaluate the capability of the PHysically-based Extreme Value distribution of river flows (PHEV) to reliably detect flood divides.

Results show that PHEV is consistently able to recognize the presence and absence of flood divides in a large set of case studies from the US and Germany. Possible reasons for the occurrence of a sizeable number of false positives are investigated by accounting for both the statistical uncertainty of relatively short observational records and the typical hydro-climatic variability of different river basins, which affects the information content of these limited data series. To this end, we perform a controlled experiment in which we remove the highest flow maxima in the flood frequency curves of the true positive cases and repeat the flood divide detection analysis on the shorter series, showing that PHEV can foresee the emergence of true flood divides in more than 80% of the cases even if the shortened observations do not display them. The result supports claims of the dependability of flood divides initially classified as false positives. An investigation of the intrinsic dynamics of streamflows in the set of true and false positives further elucidates the issue. False positives are indeed preferentially found for more persistent regimes (87% of the false positives have persistency index above two, as opposed to only 11% of true positives; the overall number of cases with persistency index above two is 55) which, by their nature, rarely exhibit large extreme flow values. The limited length of the available observed time series might be thus constraining the possibility to observe expected flood divides, analogously to what occurs when we artificially reduce the size of the observational sample.

The present analysis, performed on a wide set of catchments characterized by different hydroclimatic features, reveals PHEV as a reliable tool to identify and foresee the occurrence of flood divides and consequently unveil the propensity of rivers to large floods. The method

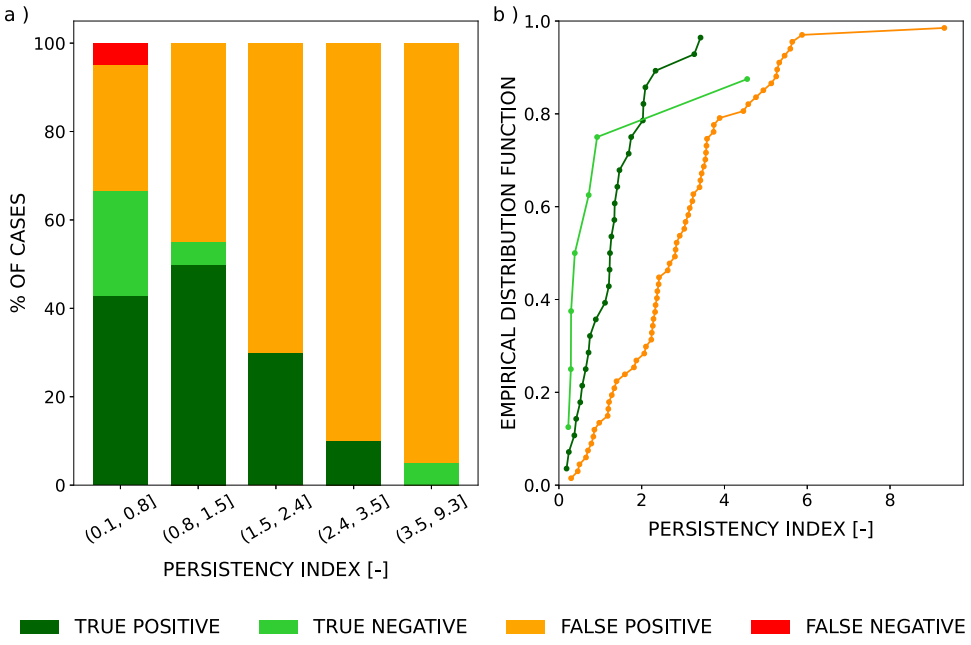

Fig. 5. (a) Performance of the PHysically-based Extreme Value (PHEV) distribution of river flows in the detection of flood divides as a function of the persistency index. Ranges (whose boundaries are reported in the x-axis) were set so as to have an equal number of values (~20) per bin. (b) Empirical cumulative distribution functions of the persistency index for true positive (dark green), true negative (light green) and false positive (orange) cases. The distributions of true versus false cases are significantly different in a statistical sense (the *p*-value of the 2-samples Kolmogorov–Smirnov test is lower than 0.01.). (For interpretation of the references to color in this figure legend, the reader is referred to the web version of this article.)

is especially relevant in data scarce conditions, although limitations linked to the domain of applicability of this tools exist and have been recalled in this work. The study lays the foundations for a better comprehension of climate and landscape controls of observed marked rises of the magnitude of the rarer floods, which is the subject of ongoing research.

CRediT authorship contribution statement

Arianna Miniussi: Conceptualization, Methodology, Software, Formal analysis, Writing – original draft, Writing – review & editing, Visualization, Project administration. **Ralf Merz:** Conceptualization, Methodology, Writing – review & editing, Funding acquisition. **Lisa Kaule:** Methodology, Software, Writing – review & editing. **Stefano Basso:** Conceptualization, Methodology, Supervision, Writing – original draft, Writing – review & editing, Funding acquisition, Project administration.

Declaration of competing interest

The authors declare that they have no known competing financial interests or personal relationships that could have appeared to influence the work reported in this paper.

Data availability

Data are freely accessible online as indicated in the Acknowledgments

Acknowledgments

This work is funded by the Deutsche Forschungsgemeinschaft (DFG, German Research Foundation) - Project Number 421396820 ‘Propensity of rivers to extreme floods: climate-landscape controls and early detection (PREDICTED)’ and Research Group FOR 2416, Germany ‘Space-Time Dynamics of Extreme Floods (SPATE)’. The financial support of the Helmholtz Centre for Environmental Research - UFZ, Germany is as well acknowledged. We thank the Bavarian State Office of Environment (LfU, https://www.gkd.bayern.de/de/fluesse/abfluss) and the Global Runoff Data Centre (GRDC) prepared by the Federal Institute for Hydrology (BfG, http://www.bafg.de/GRDC) for providing the discharge data for Germany. The MOPEX dataset is available at https://hydrology.nws.noaa.gov/pub/gcip/mopex/US_Data/. 30-year normal precipitation gridded data for the US are provided by the PRISM Climate Group, Oregon State University, http://prism.oregonstate.edu (downloaded on June, 1st 2021); 30-year normal precipitation gridded data for Germany are provided by the Deutsche Wetter Dienst (DWD) at https://opendata.dwd.de/climate_environment/CDC/grids_germany/multi_annual/precipitation/

Appendix A. Supplementary data

Supplementary material related to this article can be found online at https://doi.org/10.1016/j.jhydrol.2022.128989. It includes additional information about the study dataset, details on the performance metrics employed and some supplementary figures.

References

Allamano, P., Laio, F., Claps, P., 2011. Effects of disregarding seasonality on the distribution of hydrological extremes. Hydrol. Earth Syst. Sci. 15, 3207–3215. http://dx.doi.org/10.5194/hess-15-3207-2011.

Baratti, E., Montanari, A., Castellarin, A., Salinas, J.L., Viglione, A., Bezzi, A., 2012. Estimating the flood frequency distribution at seasonal and annual time scales. Hydrol. Earth Syst. Sci. 16, 4651–4660. http://dx.doi.org/10.5194/hess-16-4651-2012.

Basso, S., Botter, G., Merz, R., Miniussi, A., 2021. PHEV! the physically-based extreme value distribution of river flows. Environ. Res. Lett. 16, 124065. http://dx.doi.org/10.1088/1748-9326/ac3d59.

Basso, S., Frascati, A., Marani, M., Schirmer, M., Botter, G., 2015a. Climatic and landscape controls on effective discharge. Geophys. Res. Lett. 42, 8441–8447. http://dx.doi.org/10.1002/2015GL066014.

Basso, S., Schirmer, M., Botter, G., 2015b. On the emergence of heavy-tailed streamflow distributions. Adv. Water Resour. 82, 98–105. http://dx.doi.org/10.1016/j.advwatres.2015.04.013.

Basso, S., Schirmer, M., Botter, G., 2016. A physically based analytical model of flood frequency curves. Geophys. Res. Lett. 43 (17), 9070–9076. http://dx.doi.org/10.1002/2016GL069915.

Berghuijs, W.R., Sivapalan, M., Woods, R.A., Savenije, H., 2014. Patterns of similarity of seasonal water balances: A window into streamflow variability over a range of time scales. Water Resour. Res. 50, 5638–5661. http://dx.doi.org/10.1002/2014WR015692.

Bernardara, P., Schertzer, D., Eric, S., Tchiguirinskaia, I., Lang, M., 2008. The flood probability distribution tail: How heavy is it? Stoch. Environ. Res. Risk Assess. 22, 107–122. http://dx.doi.org/10.1007/s00477-006-0101-2.

Biswal, B., Marani, M., 2010. Geomorphological origin of recession curves. Geophys. Res. Lett. 37 (24), http://dx.doi.org/10.1029/2010GL045415, L24403.

Botter, G., Basso, S., Rodriguez-Iturbe, I., Rinaldo, A., 2013. Resilience of river flow regimes. Proc. Natl. Acad. Sci. 110 (32), 12925–12930. http://dx.doi.org/10.1073/pnas.1311920110.

Botter, G., Porporato, A., Rodriguez-Iturbe, I., Rinaldo, A., 2007. Basin-scale soil moisture dynamics and the probabilistic characterization of carrier hydrologic flows: Slow, leaching-prone components of the hydrologic response. Water Resour. Res. 43 (2), http://dx.doi.org/10.1029/2006WR005043.

Botter, G., Porporato, A., Rodriguez-Iturbe, I., Rinaldo, A., 2009. Nonlinear storage-discharge relations and catchment streamflow regimes. Water Resour. Res. 45 (10), http://dx.doi.org/10.1029/2008WR007658.

Brutsaert, W., Nieber, J.L., 1977. Regionalized drought flow hydrographs from a mature glaciated plateau. Water Resour. Res. 13 (3), 637–643. http://dx.doi.org/10.1029/WR013i003p00637.

Budyko, M., 1974. Climate and Life. Academic Press, New York.

Cohen, J., 1974. Statistical Power Analysis for the Behavioral Sciences. Lawrence Erlbaum Associates.

Deal, E., Braun, J., Botter, G., 2018. Understanding the role of rainfall and hydrology in determining fluvial erosion efficiency. J. Geophys. Res. Earth Surface 123 (4), 744–778. http://dx.doi.org/10.1002/2017JF004393.

Duan, Q., Shaake, J., Andreassian, V., S., F., Goteti, G., Gupta, H., Y.M., G., Habets., F., Hall., A., Hay., L., Hoguek., T., Huang., M., Leavesley, G., Liang., X., Nasonova., O., Noilhanh., J., Oudinc, S., Sorooshian., T., Wagener, E., Wood., E., 2005. Model parameter estimation experiment (MOPEX): An overview of science strategy and major results from the second and third workshops. J. Hydrol. 320, 3–17. http://dx.doi.org/10.1016/j.jhydrol.2005.07.031.

Farquharson, F.A.K., Meigh, J.R., Sutcliffe, J., 1992. Regional flood frequency analysis in arid and semi-arid areas. J. Hydrol. 138 (3), 487–501. http://dx.doi.org/10.1016/0022-1694(92)90132-F.

Gaume, E., 2006. On the asymptotic behavior of flood peak distributions. Hydrol. Earth Syst. Sci. 10, 233–243.

Gignac, G.E., Szodorai, E.T., 2016. Effect size guidelines for individual differences researchers. Pers. Individ. Differ. 102, 74–78. http://dx.doi.org/10.1016/j.paid.2016.06.069.

Guo, J., Li, H.-Y., Leung, L.R., Guo, S., Liu, P., Sivapalan, M., 2014. Links between flood frequency and annual water balance behaviors: A basis for similarity and regionalization. Water Resour. Res. 50, http://dx.doi.org/10.1002/2013WR014374.

Hirschboeck, K., 1987. Hydroclimatically-defined mixed distributions in partial duration flood series. In: Singh, V.P. (Ed.), Hydrologic Frequency Modeling. Springer, Louisiana State University, Dordrecht, Baton Rouge, U.S.A, pp. 199–212.

Jianchun, L., Pope, G.A., Sepehrnoori, K., 1995. A high-resolution finite-difference scheme for nonuniform grids. Appl. Math. Model. 19 (3), 162–172. http://dx.doi.org/10.1016/0307-904X(94)00020-7.

Laio, F., Porporato, A., Ridolfi, L., Rodriguez-Iturbe, I., 2001. Plants in water-controlled ecosystems: active role in hydrologic processes and response to water stress: II. Probabilistic soil moisture dynamics. Adv. Water Resour. 24 (7), 707–723. http://dx.doi.org/10.1016/S0309-1708(01)00005-7.

Lovakov, A., Agadullina, E.R., 2021. Empirically derived guidelines for effect size interpretation in social psychology. Eur. J. Soc. Psychol. 51 (3), 485–504. http://dx.doi.org/10.1002/ejsp.2752.

Mann, H.B., Whitney, D.R., 1947. On a Test of Whether one of Two Random Variables is Stochastically Larger than the Other. Ann. Math. Stat. 18 (1), 50–60. http://dx.doi.org/10.1214/aoms/1177730491.

Merz, B., Basso, S., Fischer, S., Lun, D., Blöschl, G., Merz, R., Guse, B., Viglione, A., Vorogushyn, S., Macdonald, E., Wietzke, L., Schumann, A., 2022. Understanding heavy tails of flood peak distributions. Water Resour. Res. 58 (6), http://dx.doi.org/10.1029/2021WR030506, e2021WR030506.

Merz, R., Blöschl, G., 2003. A process typology of regional floods. Water Resour. Res. 39, 9578–9591. http://dx.doi.org/10.1029/2002WR001952.

Merz, B., Blöschl, G., Vorogushyn, S., et al., 2021. Causes, impacts and patterns of disastrous river floods. Nat. Rev. Earth Environ. 2, 592–609. http://dx.doi.org/10.1038/s43017-021-00195-3.

Merz, R., Tarasova, L., Basso, S., 2020. Parameter's controls of distributed catchment models—How much information is in conventional catchment descriptors? Water Resour. Res. 56 (2), http://dx.doi.org/10.1029/2019WR026008, e2019WR026008.

Merz, B., Vorogushyn, S., Lall, U., Viglione, A., Blöschl, G., 2015. Charting unknown waters — On the role of surprise in flood risk assessment and management. Water Resour. Res. 51, 6399–6416. http://dx.doi.org/10.1002/2015WR017464.

Mushtaq, S., Miniussi, A., Merz, R., Basso, S., 2022. Reliable estimation of high floods: A method to select the most suitable ordinary distribution in the metastatistical extreme value framework. Adv. Water Resour. 161, 104127. http://dx.doi.org/10.1016/j.advwatres.2022.104127.

Porporato, A., Daly, E., Rodriguez-Iturbe, I., 2004. Soil water balance and ecosystem response to climate change. Amer. Nat. 164, 625–632. http://dx.doi.org/10.1086/424970.

Rogger, M., Pirkl, H., Viglione, A., Komma, J., Kohl, B., Kirnbauer, R., Merz, R., Blöschl, G., 2012. Step changes in the flood frequency curve: process controls. Water Resour. Res. 48, W05544. http://dx.doi.org/10.1029/2011WR011187.

Rogger, M., Viglione, A., Derx, J., Blöschl, G., 2013. Quantifying effects of catchments storage thresholds on step changes in the flood frequency curve. Water Resour. Res. 49, 6946–6958. http://dx.doi.org/10.1002/wrcr.20553.

Schaake, J., Duan, Q., Andréassian, V., Franks, S., Hall, A., Leavesley, G., 2006. The model parameter estimation experiment (MOPEX). J. Hydrol. 320 (1), 1–2. http://dx.doi.org/10.1016/j.jhydrol.2005.07.054, The model parameter estimation experiment.

Smith, J.A., Cox, A.A., Baeck, M.L., Yang, L., Bates, P.D., 2018. Strange floods: The upper tail of flood peaks in the United States. Water Resour. Res. 54, 6510–6542. http://dx.doi.org/10.1029/2018WR022539.

Sullivan, G., Feinn, R., 2012. Using effect size — or why the p value is not enough. J. Graduate Med. Educ. 279–282. http://dx.doi.org/10.4300/JGME-D-12-00156.1.

Tarasova, L., Basso, S., Merz, R., 2020. Transformation of generation processes from small runoff events to large floods. Geophys. Res. Lett. 47 (22), http://dx.doi.org/10.1029/2020GL090547, e2020GL090547.

Tarasova, L., Basso, S., Zink, M., Merz, R., 2018. Exploring controls on rainfall-runoff events: 1. Time series-based event separation and temporal dynamics of event runoff response in Germany. Water Resour. Res. 54, 7711–7732. http://dx.doi.org/10.1029/2018WR022587.

Villarini, G., Smith, J., 2010. Flood peak distributions for the eastern United States. Water Resour. Res. 46, http://dx.doi.org/10.1029/2009WR008395.

Wallemacq, P., House, R., 2018. Economic Losses, Poverty & Disasters 1998–2017. Technical Report, United Nations Office for Disaster Risk Reduction (UNDRR) and Centre for Research on the Epidemiology of Disasters (CRED).

Wang, D., Hejazi, M., 2011. Quantifying the relative contribution of the climate and direct human impacts on mean annual streamflow in the contiguous United States. Water Resour. Res. 47, http://dx.doi.org/10.1029/2010WR010283.